Developmental Biology 500 (2023) 31–39

Contents lists available at ScienceDirect

Developmental Biology

journal homepage: www.elsevier.com/locate/developmentalbiology

Downregulation of *Yap1* during limb regeneration results in defective bone formation in axolotl

Sadık Bay [a,b,**], Gürkan Öztürk [a,c], Nesrin Emekli [d], Turan Demircan [e,f,*]

[a] Regenerative and Restorative Medicine Research Center (REMER), Research Institute for Health Sciences and Technologies (SABITA), Istanbul Medipol University, Istanbul, 34810, Turkey
[b] Graduate School of Health Sciences, İstanbul Medipol University, İstanbul, Turkey
[c] Department of Physiology, International School of Medicine, Istanbul Medipol University, Istanbul, Turkey
[d] Department of Medical Biochemistry, Faculty of Medicine, Istanbul Medipol University, Istanbul, Turkey
[e] Department of Medical Biology, School of Medicine, Muğla Sıtkı Koçman University, Muğla, Turkey
[f] Department of Bioinformatics, Muğla Sıtkı Koçman University, Muğla, Turkey

ARTICLE INFO

Keywords:
YAP1
Hippo pathway
Axolotl
Regeneration
Proteomics
Bone formation defect

ABSTRACT

The Hippo pathway plays an imperative role in cellular processes such as differentiation, regeneration, cell migration, organ growth, apoptosis, and cell cycle. Transcription coregulator component of Hippo pathway, YAP1, promotes transcription of genes involved in cell proliferation, migration, differentiation, and suppressing apoptosis. However, its role in epimorphic regeneration has not been fully explored. The axolotl is a well-established model organism for developmental biology and regeneration studies. By exploiting its remarkable regenerative capacity, we investigated the role of *Yap1* in the early blastema stage of limb regeneration. Depleting *Yap1* using gene-specific morpholinos attenuated the competence of axolotl limb regeneration evident in bone formation defects. To explore the affected downstream pathways from *Yap1* down-regulation, the gene expression profile was examined by employing LC-MS/MS technology. Based on the generated data, we provided a new layer of evidence on the putative roles of increased protease inhibition and immune system activities and altered ECM composition in diminished bone formation capacity during axolotl limb regeneration upon *Yap1* deficiency. We believe that new insights into the roles of the Hippo pathway in complex structure regeneration were granted in this study.

1. Introduction

The Hippo pathway regulates multiple cellular processes, including organ growth, cell proliferation, apoptosis, the transmission of mechanical signals, cell cycle, cell migration, differentiation, organ and limb regeneration (Hayashi et al., 2015; Moya and Halder, 2018; Panciera et al., 2017). This pathway also cross-talks with other signaling pathways such as Wnt (Wingless/Ints), GPCRs (G-Protein Coupled Receptors), RTKs (Receptor Tyrosin Kinases) (Moya and Halder, 2018) to function in organ development and homeostasis. Accumulated studies in mammals and highly regenerative model organisms have demonstrated that misregulation of the Hippo pathway affects a wide range of biological processes and pathology of the diseases.

In addition to its regulatory roles during embryonic development, the Hippo signaling pathway controls organ size maintenance following the tissue or organ regeneration in animals. During mouse embryogenesis, deletion of the *MST1* and *MST2* kinase genes showed enlargement of the liver and heart (Camargo et al., 2007; Dong et al., 2007). Previous studies have suggested that the apparent diminish in cardiac regeneration capacity of mammals a few days after birth is due to the decrease in the transcriptional activity of *YAP1*, which is negatively regulated by increased activity of the tumor suppressor proteins LATS1 and LATS2 (Heallen et al., 2013; Xin et al., 2013). In another study conducted in adult mice, a high level of *YAP1* was associated with liver enlargement (Benhamouche et al., 2010). In mammals, albeit with limited regeneration capacity, there is accumulating evidence for the induction of tissue repair upon *YAP/TAZ* activation in different tissues. Previous findings have linked intestinal regeneration with *YAP1* activity. After an intestinal

* Corresponding author. Department of Medical Biology, School of Medicine, Muğla Sıtkı Koçman University, Muğla, Turkey.
** Corresponding author. Regenerative and Restorative Medicine Research Center (REMER), Research Institute for Health Sciences and Technologies (SABITA), Istanbul Medipol University, Istanbul, 34810, Turkey.
E-mail addresses: sbay@medipol.edu.tr (S. Bay), turandemircan@mu.edu.tr (T. Demircan).

https://doi.org/10.1016/j.ydbio.2023.06.001
Received 5 February 2022; Received in revised form 25 May 2023; Accepted 1 June 2023
Available online 2 June 2023

injury, the inhibitory phosphorylation of *YAP1* by the upstream kinases is lifted, and the active *YAP1* is translocated to the nucleus. After this localization, the transcriptional activity provided by *YAP1* initiates the stem cell self-renewal programming directed by the Wnt pathway (Gregorieff et al., 2015; Yui et al., 2018). Moreover, enrichment of *YAP1* in the LGR5+ stem cell compartment of the intestinal crypt during homeostasis and its upregulation during regeneration (Cai et al., 2010) highlighted the active participation of *YAP1* in these processes. As in the intestine, the regeneration program in the liver requires activation of *YAP1*, which is evident by the enhancement of liver regeneration consequent to experimental activation of *YAP1* (Bai et al., 2012), even in aged mice with an impaired liver regeneration potential (Loforese et al., 2017). Increased proliferation of embryonic cardiomyocytes following *YAP1* activation resulted in a continuous proliferation of cardiomyocytes in adults, which might be the key to enabling heart function restoration after infarction (von Gise et al., 2012). In addition to these organs, *YAP1* also plays essential roles in skin regeneration, as evident in the previous studies where the silencing of *YAP/TAZ* gene expression interferes with skin cell proliferation and successful skin regeneration in mammals (Johnson and Halder, 2014; Juan and Hong, 2016). The observed regulatory functions of *YAP1* in flatworms' whole-body regeneration highlights the necessity of the *YAP1* activity in the regeneration process of invertebrates (Demircan and Berezikov, 2013; Lin and Pearson, 2014). Furthermore, studies in different model systems have exhibited that the Hippo pathway role in organ regeneration is highly conserved among animals (Hayashi et al., 2015).

Amphibians, unlike other tetrapods, display a higher organ and tissue regeneration ability (Nye et al., 2003) extended to complete regeneration of many organs and extremities such as the cornea, lens, retina, heart, spinal cord, brain, tail, and limb (Stocum, 2006). Axolotl, a fruitful model organism for developmental biology and regeneration studies, has a high regeneration capacity throughout its life due to larval-like characteristics in adulthood as it can not undergo metamorphosis naturally (Galliot and Ghila, 2010). Therefore, it is a widely utilized model to study the molecular mechanisms of regeneration, particularly to explore the key steps of and regulators in limb regeneration. Furthermore, as another remarkable experimental advantage, axolotls can be induced to metamorphosis by thyroid hormone administration, which allows researchers to evaluate the limb regeneration capacity at different developmental stages during adulthood (Rosenkilde et al., 1982). Initial reports indicating the drastic drop of regeneration capacity and fidelity upon metamorphosis suggest using pre-and post-metamorphic axolotls to expand our knowledge on limb regeneration (Demircan et al., 2018; Monaghan et al., 2014).

One of the critical cellular processes in organ regeneration is the regeneration's size control step. In axolotl and various frog species, organs return to their original size after damage (Beck et al., 2009; McCusker et al., 2015; Slack et al., 2008). As documented before, differentiated cells turn into progenitor and stem cells and accumulate at the injury site upon an injury or amputation. The formation of regeneration-specific tissue, blastema, is indispensable to renew the missing parts. Later stages of regeneration can be summarized as restoration of the limb structure and reshaping of the newly formed limb. It has been described that the YAP protein is highly active during tail and limb regeneration in *Xenopus laevis*. YAP and TEAD4 proteins are essential to maintain original size, and the absence of YAP or TEAD4 proteins during regeneration leads to a shorter tail in tadpoles (Hayashi et al., 2014a). In addition to tail regeneration, YAP protein activation was detected during *Xenopus laevis* limb regeneration (Hayashi et al., 2014b). The signaling cascades regulating renewed structure's final size in axolotl limb regeneration are not fully understood yet.

In this study, we investigated the putative roles of *Yap1* in axolotl limb regeneration. Significantly higher *Yap1* expression at mRNA and protein levels in neotenic axolotls compared to the metamorphic animals at 10 day-post amputation (dpa) prompted us to down-regulate the neotenic *Yap1* expression at the early blastema stage of limb regeneration. Microscopic, macroscopic and computational tomography (CT) based analyses revealed the defective bone regeneration due to the *Yap1* inhibition. To provide molecular clues, the proteome of *Yap1* inhibited and control animals were compared. We identified essential peptidase activity, immune system, and wound healing related pathways enriched by the differentially expressed proteins between two groups. The findings of this study will contribute to the understanding of the *Yap1* roles in successful regeneration.

2. Material and methods

2.1. Animal husbandry and ethical İssues

Axolotls 12–15 cm in size and 1 year old were used in this study. Animals were maintained in Holtfreter's solution at 18 ± 2 °C temperature as one individual in an aquarium as described in a previous study (Demircan et al., 2019) throughout the experiments. Required permission and approval for this study was obtained from the local ethics committee of animal experiments of Istanbul Medipol University (IMU-HADYEK, Approval Number: 38828770-604.01.01-E.14550).

2.2. Induction of metamorphosis

A previously established protocol (Demircan et al., 2018) was followed to induce the metamorphosis for neotenic axolotls. Briefly, randomly selected animals (n = 18) were treated with T3 (3,3′,5-Triiodo-L-thyronine – Sigma T2877) twice a week in Holtfreter's solution with a 25 nM final concentration. Morphological alterations such as weight loss, disappearance of the fin and gills were monitored carefully to follow the transition to the metamorphic stage, and approximately after 4 weeks of treatment, the T3 concentration was reduced to half. The hormone was administered for an additional two weeks. After fully metamorphosis was accomplished, animals were kept for a month without hormone treatment to allow them to adapt to the terrestrial life conditions.

2.3. Sample collection

Prior to amputations, the animals were anesthetized using 0.1% Ethyl 3-aminobenzoate methanesulfonate (MS-222, Sigma-Aldrich, St Louis, MO, USA) dissolved in Holtfreter's solution. Right forelimbs of animals were amputated at mid zeugopod level under a dissecting microscope (Zeiss - StereoV8). To compare *Yap1* mRNA levels between neotenic (n = 15) and metamorphic animals (n = 15), tissue samples were collected at the early steps of regeneration (1, 7,10,14,21 dpa). Blastema samples of neotenic (n = 3) and metamorphic (n = 3) axolotls at 10 dpa were obtained to evaluate the YAP1 protein expression level by immunohistochemistry. The efficiency of morpholino injections was assessed on blastema samples (n = 3 for *Yap1* and n = 3 for control morpholino injections) removed at 16 dpa. For proteomics and qRT-PCR experiments blastema samples were collected at 16 dpa for *Yap1* and control morpholino injected animals (n = 12 for each group). All collected tissue samples according to the defined time points were cryopreserved in liquid nitrogen and stored at −80 °C until RNA or protein isolation.

2.4. Yap1 morpholino design and administration

GeneTools (https://www.gene-tools.com/) was used to design the morpholino oligo (MO) (5′-CCTCTTACCTCAGTTACAATTTATA-3′) for *Yap1* inhibition. As a negative control, a standard oligo sequence (5′-CCTCTTACCTCAGTTACAATTTATA-3′) suggested by GeneTools was used. Morpholinos were dissolved in 2X PBS with a final concentration of 500 μM. To assess the efficiency of morpholinos, each morpholino was injected into 3 axolotls at 10 dpa. To determine the effect of morpholinos on regeneration, each morpholino was administrated to another 9 axolotls at 10 dpa. For proteomics and qRT-PCR experiments each morpholino was injected into 12 axolotls at 10 dpa. Injection into blastema

using Hamilton injector (SGE 025RN, 25 GA 50 MM) was followed by electroporation as described elsewhere (Leigh et al., 2020). Electroporation efficiency was assessed by co-injection of GFP encoding plasmid. Fluorescent imaging of blastema tissues was performed using AxioZoom V16 (Zeiss) microscope before and on the 4th and 7th day after injection.

2.5. Quantitative real-time polimerase chain reaction (qRT-PCR)

To compare the expression level of *Yap1* in neotenic and metamorphic axolotl blastema, tissue samples at 1, 7, 10, 14, and 21 were isolated (n = 15 for neotenic and metamorphic animals, and n = 3 per time point). To evaluate the efficiency of *Yap1* knockdown, blastema tissues were obtained 6 days after injection (n = 3 for *Yap1* and control morpholinos). The details of the following qRT-PCR protocol was described elsewhere(Sibai et al., 2019). Briefly, RNA from collected samples was isolated using the Total RNA Purification Kit (Norgen-Biotek, 37500) according to the manufacturer's protocol. The quality of isolated RNA was checked on 1% agarose gel. The quantity of RNA was measured using the nanodrop. ProtoScript First Strand cDNA Synthesis Kit (NEB, E6300S) was employed following the producer's procedure to synthesize the complementary DNA starting with 1 μg total RNA. SensiFAST™ SYBR® No-ROX Kit (Bioline, BIO98005) was utilized in qPCR, considering the manufacturer's suggestions. Primer sequences to amplify *Yap1* and *Elf1α* (housekeeping gene used for normalization) were provided in Table S1 qPCR experiments were performed in 3 biological and 3 technical replicates and CFX Connect-Real Time System (BIO RAD) device was used for this reaction. With $2^{-\Delta\Delta Ct}$ method, relative messenger RNA (mRNA) expressions were calculated.

2.6. Immunofluorescent (IF) staining

To label the YAP protein in axolotl blastema tissues, a protocol used in *Xenopus laevis* (Hayashi et al., 2014b) was slightly modified and used. Blastema tissues (n = 3 for neotenic and metamorphic animals) were first embedded in a tissue freezing medium (Leica, 14020108926). Then, the embedded tissues were placed on a Cryostat device (Leica, CM1950) for sectioning to get the slices with 25 μm thickness. The sections were placed on positively charged slides (Superfrost Plus, ThermoScientific, J1800AMNZ) and outlined with a PAP-PEN (Invitrogen, 008877). Later, sections were fixed 2 times with 4% PFA (Sigma, 158127) for 15 min followed by subsequent incubation steps in 0.1% Triton TX-100 (Sigma, T8787) for 20 min, 0.3% H_2O_2 (Sigma, H1009) for 10 min, and 2% FBS (ThermoFisher Scientific, 16140071) for 1 h. Primary Rabbit-anti-YAP antibody (Cell Signalling Technology - 4912) diluted 1:250 was added to cover the samples on slides and an overnight incubation at +4 °C was followed. Samples were incubated with Alexa Fluor 594 attached Goat-anti-Rabbit secondary antibody (Invitrogen, A11037, diluted 1:250) for 3 h at room temperature. After the DAPI (Sigma, D9542) with 1:1000 dilution was added to stain the nucleus, slides were covered with the mounting solution (Mounting Medium, C9368). For imaging, a confocal microscope (Zeiss LSM800 with AiryScan) was used. As a negative control, slides stained with secondary antibody only were imaged. Antibody positive cells in tissues were counted with ZenBlue (Zeiss) software.

2.7. Computational tomography (CT)

U-CT (MiLabs) device was used to determine whether bone development was affected by *Yap1* inhibition during limb regeneration (n = 9 for control and *Yap1* morpholino injections). After the axolotls were anesthetized, they were placed in a tomography container suitable for the size of the analyzed animals. High-resolution scan mode was selected for imaging, and the 'Reconstitution (MiLabs)' software of the device was utilized to convert the images to 3D. The data was transferred to the 'IMALYTICS Preclinical 2.1 (MiLabs)' software for further processing to adjust the brightness and contrast.

2.8. Proteomics analysis by LC-MS

Animals (n = 24) were randomly divided into two groups and amputated as described above. At the early blastema stage (10 dpa), *Yap1* and control morpholinos were administrated to *Yap1*-KD or the control groups following the procedure described before. One week after the morpholino injections, 9 blastema tissues for each treatment were collected and gathered to form three replicates, in which three samples were pooled. For proteomics analysis, previously established protocols were followed (Cevik et al., 2016; Sibai et al., 2020). Briefly, mortar and pestle were used to powder the frozen blastema samples for protein extraction. Proteins were isolated using an ultrasonic homogenizer with three 5s on- 5 s off cycles and quantified by Qubit 4.0. Filter-aided sample preparation (FASP) (Abcam - ab270519) method was applied to obtain the tryptic peptides, and the mixture of 500 ng tryptic peptides was used in triplicates in downstream steps. ACQUITY UPLC (Waters) chromatography coupled high-resolution mass spectrometry SYNAPTG2-Si (Waters) system was used for the analysis of peptides. The parameters defined in previous studies (Cevik et al., 2016; Sibai et al., 2020) were followed for peptide separation and MSE data collection. Obtained signals were preprocessed with ProteinLynx Global Server (v2.5, Waters) and a previously generated axolotl database (Demircan et al., 2017) was used to identify and review the peptide sequences. Progenesis QI for proteomics (v.4.0, Waters) software was employed for protein identification and quantitative analysis of detected peptides. Normalization of data was conducted according to the relative quantitation of non-conflicting peptides. ANOVA test was applied to filter the proteins with a p-value ≤ 0.01 and a 2-fold or greater differential expression level between the two conditions. To validate the proteomics results and evaluate the expression level of the genes with osteogenic or chondrogenic activity, 6 blastema tissues the RT-qPCR method described above was applied using the gene-specific primers (Table S1) *Yap1*-KD treatment (n = 3) and control samples (n = 3).

2.9. Enrichment of gene ontology (GO) terms and KEGG pathways

Differentially enriched (DE) proteins between the *Yap1* morpholino treated and control groups were tested for identifying Molecular function (MF), biological process (BP), and cellular component (CC) GO terms using "clusterProfiler" package in R (Yu et al., 2012a). The same package was used to explore the Kyoto Encyclopedia of Genes and Genomes (KEGG) pathways enriched by DE proteins. The parameters applied for enrichment analyses were as follows: p-value and q-value cutoffs were 0.05, and adjusted p-value was Benjamini & Hochberg (BH). Enriched GO terms and pathways were visualized on dot plot and bar plot graphs using the "ggplot2" package in R.

2.10. Statistics

GraphPad Prism 8 (San Diego, CA, USA) was used for statistical analysis. In order to test the normality of data distribution, the Shapiro-Wilk test was carried out. One-way ANOVA with post-hoc Tukey's test was applied on qRT-PCR and proteomics data. The chi-squared test was employed in the percentages calculated of IF results. The student's t-test was used to compare the limb measurement results. All p-values smaller than 0.05 were considered significant. An asterisk (*), two asterisks (**) or three asterisks (***) were used to indicate the significance of p values as follows: $0.05 \leq$p-value≤ 0.01, $0.01 <$p-value≤ 0.001 or p<0.001, respectively.

3. Results

3.1. Neotenic Yap1 mRNA and protein levels were higher than metamorphic Yap1 in blastema

Considering the decreased regeneration capacity in metamorphic

axolotls, we first compared the *Yap1* level in neotenic and metamorphic blastema tissues at 1, 7, 10, 14, and 21 dpa to inspect the putative link between *Yap1* and limb regeneration potential by employing the qRT-PCR (Fig. S1, Fig. 1A). Although a higher expression level of *Yap1* was detected in neotenic tissues compared to metamorphic ones at all time points, the greatest expression level difference was identified at 10 dpa. Furthermore, the highest expression level of *Yap1* in neotenic axolotls was detected at 14 dpa (Fig. S1A). *Yap1* was substantially and significantly upregulated in neotenic blastema tissue compared to metamorphic one at mRNA level (>70x) (Fig. 1A). This finding was further validated by IF results, where the rate of *Yap* positive cells in neotenic blastema tissue was higher than the metamorphic samples (Fig. 1B) (13,12% and 3.03%, respectively). According to these results, *Yap1* levels were elevated at both mRNA and protein levels in neotenic animals in comparison to metamorphic ones at the early blastema stage of axolotl limb regeneration.

3.2. An efficient knock-down of Yap1 was achieved by morpholino i?njection

Since the expression level of *Yap1* continued to increase after 10 dpa (Fig. S1A), this blastema time point was selected for morpholino injection. To inhibit the *Yap1* activity in blastema tissue, its mRNA was depleted using a designed gene-specific morpholino. Since The efficiency of morpholino on *Yap1* expression was tested by qRT-PCR and IF methods (Fig. 1C and D). Morpholinos were injected at 10dpa and mRNA level, and the rate of YAP + cells was evaluated 2 and 6 days after administration of morpholino, respectively. The Yap-MO injected group (*Yap1*-KD) had a significantly reduced *Yap1* mRNA level (3.48x) compared to the control-MO injected group (Fig. 1C). The rate of YAP-positive cells in the Yap-MO injected group was detected significantly lower than the control-MO injected group (Fig. 1D) (6.49% and 20.89%, respectively). Hence, we concluded that Yap-MO was effective in inhibiting the *Yap1* activity, and we, therefore, used this MO in subsequent experiments.

3.3. Yap1 inhibition interfered with successful bone regeneration in axolotl

After the Yap-MO injection animals were followed for long-term macroscopic and microscopic observations. Blastema measurements at 1-week post-injection indicated a significant decrease in blastema size between Yap-MO and control-MO injected animals (Fig. 2A and B). Macroscopic observations did not unveil any detectable morphological differences between the groups at 52 dpa (Fig. 2A). However, observed softer digit formation in the renewed limb prompted us to analyze the bone structure employing the Micro-CT at 52 dpa. Bone defects due to bone orientation disorder and bone loss were detected for YAP-MO injected axolotls (Fig. 2C), highlighting the roles of YAP1 protein in successful bone development and regeneration in the axolotl.

3.4. Proteomics results highlighted that Yap1 down-regulation altered the essential downstream pathways

In order to reveal the molecular mechanisms affected by *Yap1* down-regulation, proteomics was performed for Yap-MO and control-MO administered groups. By having 3-fold decrease at the protein level after 6 days of morpholino injections (Fig. 1D), proteomics analysis was carried out 6 days after the morpholino injections, at 16 dpa. Comparison of gene expression levels in blastema at 16dpa resulted in 903 identified and 285 differentially expressed (DE) proteins (Table S2). Proteomics results were validated by RT-qPCR (Fig. 3A). The observed correlation between proteomics and RT-qPCR results prompted us to continue with downstream analyses. Among these proteins, 472 (208 significant) proteins were upregulated in the Yap-MO group, whereas 431 (77 significant) genes were downregulated. Alpha-2-HS-glycoprotein (AHSG), regulator of G-protein signaling 18 (RGS18), and complement component C3 (*C3*) genes were the top significantly upregulated genes, while peptidyl-prolyl cis-trans isomerase (FKBP2), Glutathione S-transferase M1 (GSTM1), and ATPase H + Transporting V1 Subunit G1 (ATP6V1G1) genes were detected as top downregulated genes. DE proteins were used to enrich the GO terms, KEGG pathways, and GSEA terms.

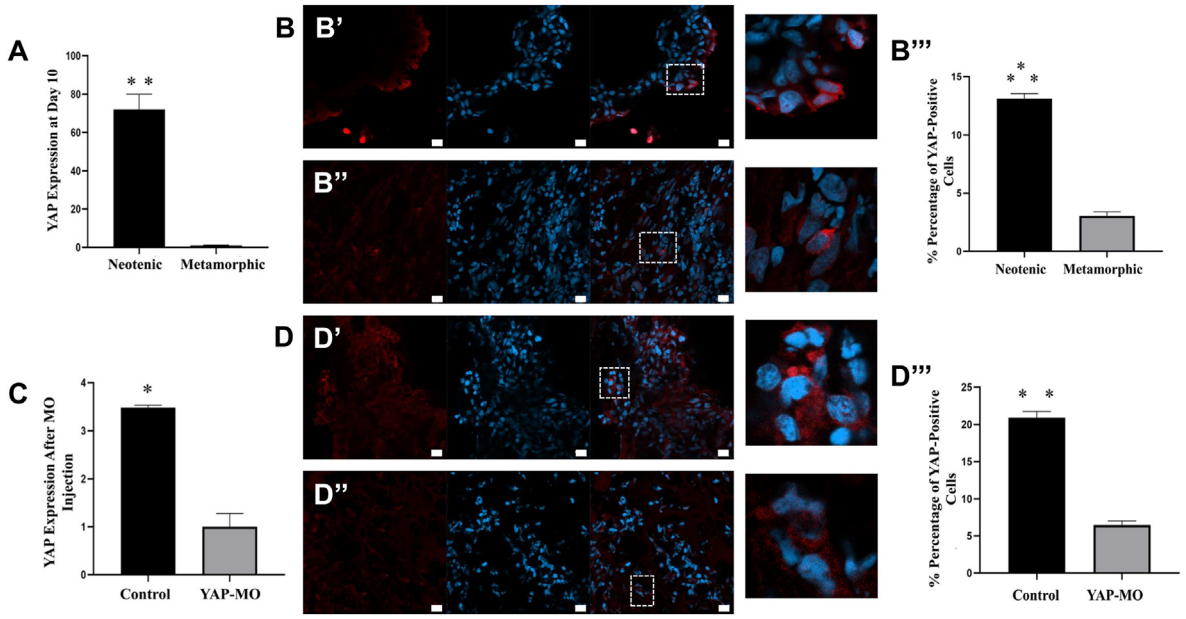

Fig. 1. *Yap1* was downregulated during axolotl limb regeneration using morpholino (MO). Neotenic axolotl *Yap1* mRNA expression levels were 72 times more compared to metamorphic *Yap1* mRNA expression at 10 days post amputation (dpa) (A) ($0.01<p^{**}\leq 0.001$). For determining YAP1 protein level, neotenic (B′) and metamorphic (B″) blastema tissues were stained with YAP1 antibody at 10 dpa (B). Percentage of YAP1-positive cells was 13,12% in neotenic axolotl while percentage of YAP1-positive cells was 3,03% in metamorphic axolotl at 10 dpa (B‴) ($p^{***}<0.001$). YAP-MO were synthesized for inhibition of axolotl *Yap1* mRNAs. After MO injection to blastema tissue of neotenic axolotl at 10 dpa, qRT-PCR analysis were performed at 16 dpa. *Yap1* mRNA expression in YAP-MO animals decreased 3,48 times compared to control animals (C) ($0.05\leq p^{*}\leq 0.01$). Yap1 in control axolotl (D′) and Yap-MO (D″) axolotl were imaged in blastema tissues (D). Yap-MO caused the level of Yap1 protein to decrease from 20,89% to 6,49% at 16 dpa (D‴). Scale bars represent 20 μm.

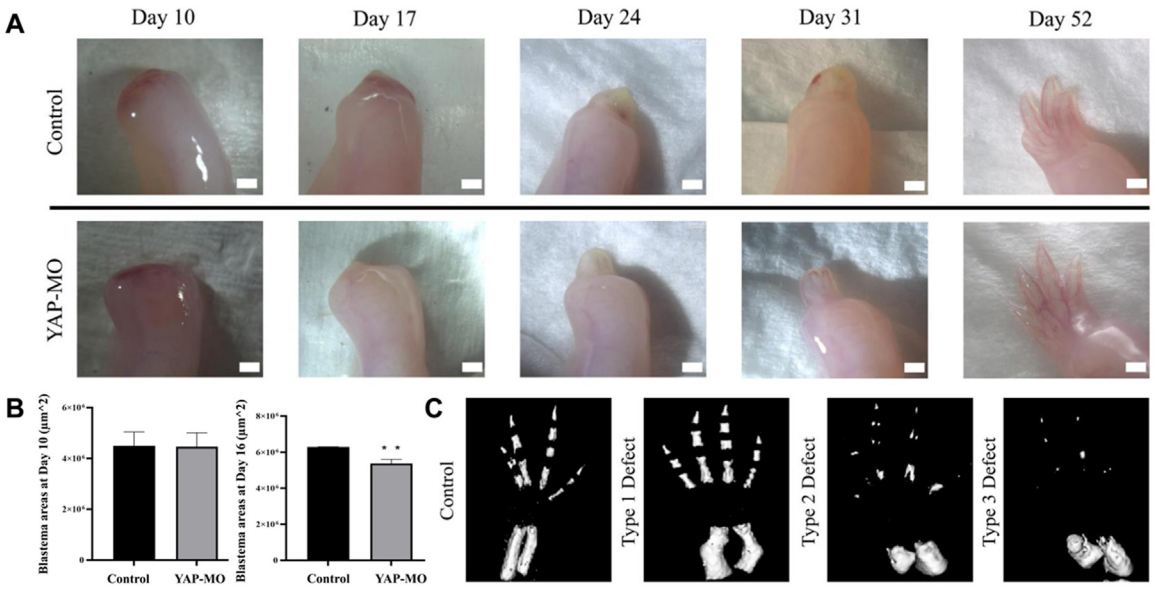

Fig. 2. YAP-MO caused bone defects during axolotl limb regeneration. After YAP-MO injection, macroscopic imaging's were performed at 10, 17, 24, 31 and 52 dpa. Different regeneration patterns were observed between control axolotls (n = 3) and YAP-MO axolotls (n = 3) as a result of long-term bright field imaging (A). Scale bars represent 1 mm. YAP-MO injection induced the decrease of blastema areas at 16 dpa. At 10 dpa, significant change was not determined between control axolotls (n = 3) and YAP-MO axolotls (n = 3). Blastema areas were decreased in YAP-MO axolotls (n = 3) compared to control axolotls (n = 3) ($0.01<p^{**}\leq 0.001$) (B). Macroscopic differences were not detected in the bright-field results after regeneration was completed. Micro-CT analysis was performed to determine whether there was a defect in bone development after YAP-MO injection at 52 dpa. Bone orientation defect and bone loss defect were imaged with Micro-CT (C).

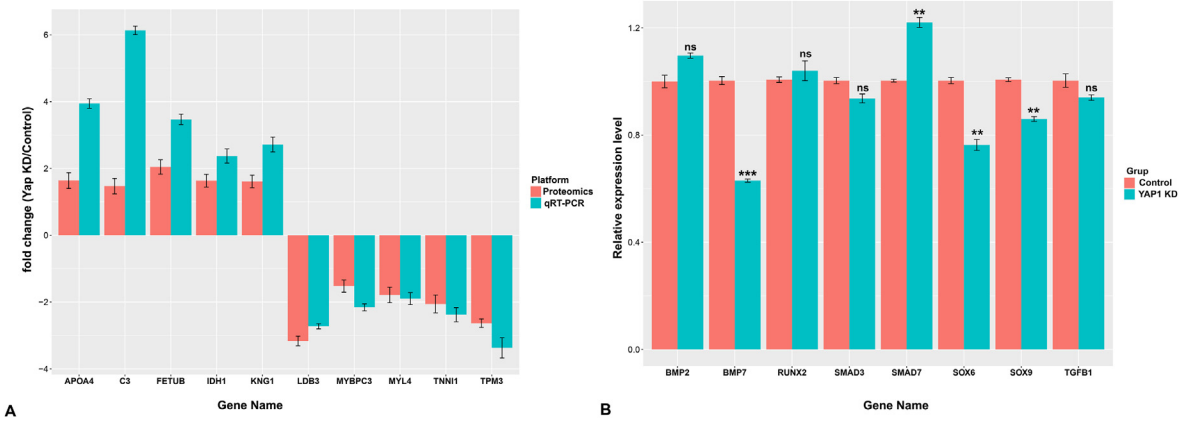

Fig. 3. Expression levels of selected genes. Among the differentially expressed genes, 10 of them were selected for validation of proteomics. Red and blue bars show the fold change based on proteomics and qRT-PCR results, respectively (A). Expression level of osteogenesis and chondrogenesis related genes was compared between control and *Yap1*-KD group (B). *p-value < 0.05, **p-value < 0.01, ***p-value < 0.001, ns; non-significant. *Apoa4*: Apolipoprotein A4, *Bmp2*: Bone morphogenetic protein 2, *Bmp4*:Bbone morphogenetic protein 4, C3: Complement component 3, *Idh1*: Isocitrate Dehydrogenase (NADP(+)) 1, *Kng1*: Kininogen-1, *Ldb3*: LIM domain binding 3, *Mybpc3*: Myosin-binding protein C 3, *Myl4*: Myosin Light Chain 4, *Prdx2*:Peroxiredoxin 2, *Runx2*: Runt-related transcription factor 2, *Smad3*: SMAD family member 3, *Smad7*: SMAD family member 3, *Sox6*: SRY-Box transcription factor 6, *Sox9*: SRY-Box transcription factor 9, *Tgfb1*: Transforming growth factor beta 1, *Tnni1*: troponin I type 1, *Tpm2*: Tropomyosin 2.

Top BP terms enriched by upregulated DE proteins such as 'regulation of endopeptidase activity', 'regulation of peptidase activity', and 'negative regulation of hydrolase activity' were related to enzymatic activities (Fig. 4A, Table S1). Upregulated DE proteins enriched 'blood microparticle', 'secretory granule lumen', and 'cytoplasmic vesicle lumen' CC terms, while 'enzyme inhibitor activity', 'endopeptidase inhibitor activity', and 'peptidase inhibitor activity' were the enriched top MF terms (Fig. 4A). On the contrary, 'muscle contraction', 'muscle system process', and 'actin filament-based movement' BP terms were detected for the downregulated DP proteins (Fig. 4B, Table S2). 'contractile fiber', 'myofibril', and 'sarcomere' were the enriched top CC terms, whereas we identified 'actin binding', 'actin filament binding', and 'extracellular matrix structural constituent' MF terms as the utmost significant terms (Fig. 4B). Enriched immune system-related BPs including 'regulation of humoral immune response', 'neutrophil activation involved in immune response', 'humoral immune response', 'acute inflammatory response', and 'complement activation' were also noticeable (Table S1, Fig. 3C). Moreover, it is noteworthy to observe that up-and down-regulated DE proteins enriched 'muscle contraction', 'actin-myosin filament sliding', 'muscle filament sliding', 'actin mediated cell contraction', and 'actin filament based movement' BPs (Fig. 4D, Table).

As a subsequent analysis, KEGG pathways were enriched by the Yap-MO upregulated and downregulated DE proteins (Fig. 5A and B, Tables S4–5). 'Complement and coagulation system', 'glutathione metabolism', and 'carbon metabolism' were detected as top KEGG pathways enriched by upregulated DE proteins. On the other hand, downregulated

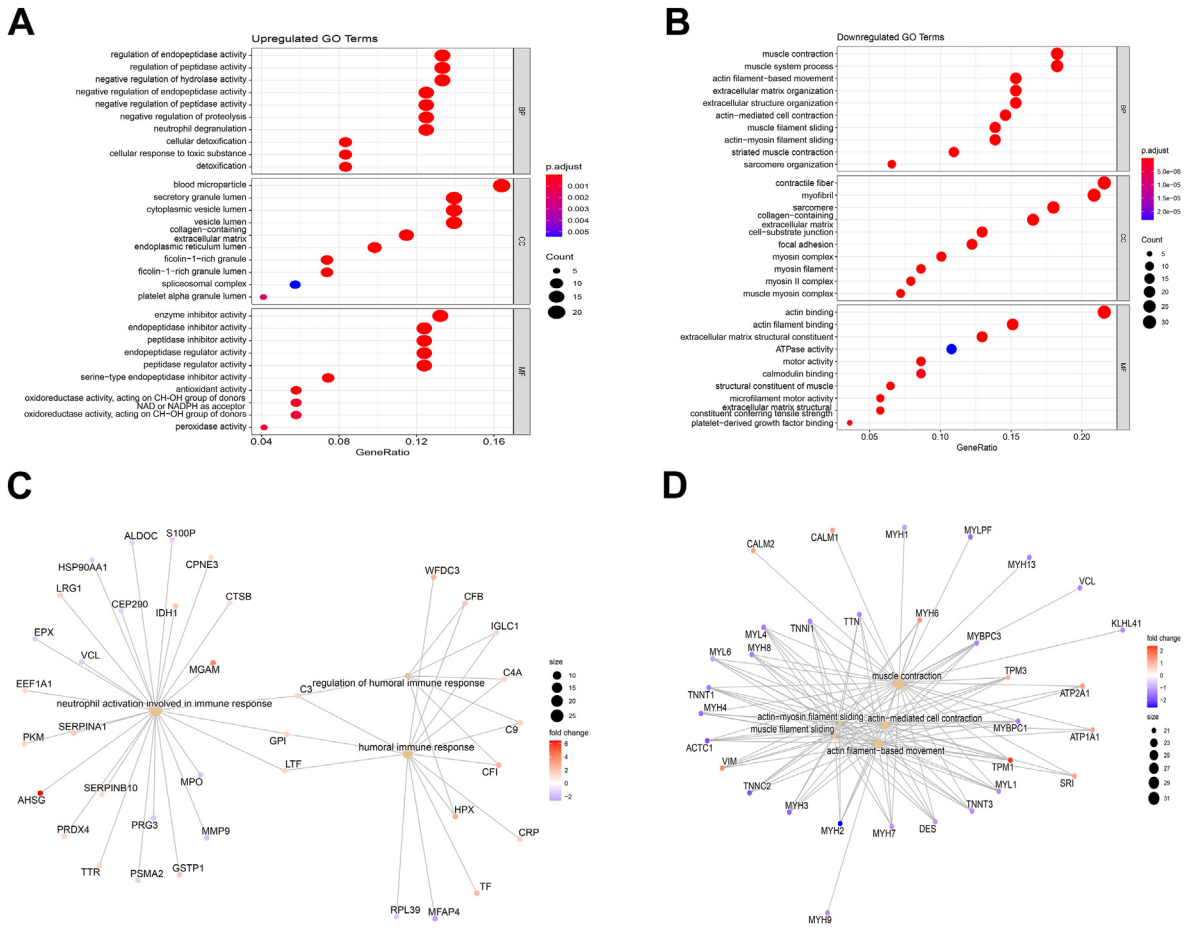

Fig. 4. Gene ontology analysis of differentially expressed proteins. (A) top 10 GO terms enriched by 208 upregulated proteins in *Yap* depleted samples compared to the control group. (B) top 10 GO terms enriched by 77 down regulated proteins in *Yap* depleted samples compared to the control group. (C) Gene-concept network of the top 3 immune-system related biological processes enriched by significantly upregulated proteins in *Yap* depleted groups. (D) Gene-concept network of the top 5 muscle system related biological processes enriched by significantly downregulated proteins in *Yap* depleted groups.

DE proteins enriched the 'focal adhesion', 'hypertrophic cardiomyopathy', and 'dilated cardiomyopathy' KEGG pathways.

Next, GO terms, and KEGG pathways were enriched using the GSEA method (Fig. 5C and D, Table S6). Top BPs were unveiled as 'Cellular process', 'biological process', and 'metabolic process' terms. 'extracellular space', 'extracellular region', and 'cytoplasm' were the top enriched CC terms, while the detected top MF terms were 'molecular function', 'binding', and 'peptidase activity'. KEGG pathways were shown on a ridgeplot and 'negative regulation of endopeptidase activity', 'negative regulation of peptidase activity', 'biological process', 'humoral response', 'inflammatory response', and 'lipid metabolic process' were the top enriched KEGG pathways (Fig. 5D). The enrichment of peptidase activity inhibition, and immune system-related pathways in the Yap-MO gene set was remarkable. GSEA based enriched GO terms, and KEGG pathways were in line with DE proteins enriched results.

Lastly, the expression levels of the key genes functioning in osteogenesis or chondrogenesis, which did not appear in our proteome data, were evaluated by qRT-PCR (Fig. 3B). Among the analyzed genes, *Sox9*, *Sox6*, and *Bmp7* were found as significantly downregulated, and *Smad7* was found to be significantly upregulated in the *Yap1* depleted group. No significant expression level differences were detected for *Tgfb-1*, *Bmp2*, and *Runx2* genes between *Yap1*_KD and control groups.

4. Discussion

The axolotl, a model organism for studying molecular mechanisms underlying regeneration, has been explored in our research for the role of YAP1 in limb regeneration (McCusker and Gardiner, 2011; McCusker et al., 2015). YAP1, an effector protein of the hippo pathway, impacts organ growth, tissue regeneration, cell proliferation, and differentiation (Kovar et al., 2020; Moya and Halder, 2018). A comparison of *Yap1* mRNA levels between metamorphic and neotenic axolotls during limb regeneration indicated increased *Yap1* expression in the latter, correlating with their superior regenerative potential (Demircan et al., 2018; Monaghan et al., 2014). As shown earlier, *Yap1* inhibition impeded bone regeneration and resulted in abnormal bone structures, thereby confirming *Yap1*'s critical role in regeneration (Hayashi et al., 2014b).

The role of YAP1 in regeneration, as demonstrated in studies on Xenopus and other model organisms (Kovar et al., 2020; Hayashi et al., 2014a, 2014b), mirrors our findings. Additionally, the critical role of *Yap1* for successful regeneration in axolotls, demonstrated by previous studies involving hydrogen peroxide-induced *Yap1* expression (Carbonell et al., 2021), validates our findings on the putative link between regeneration deficiency and YAP1 activity. Administration of YAP1 inhibitor during tail regeneration resulted in defects in appendage renewal, implying the indispensable role of *Yap1* in epimorphic regeneration.

In the context of osteogenesis, YAP1 plays an essential role in osteoblast differentiation and function. Studies have shown that the overexpression of *Yap1* can promote osteogenic differentiation, whereas its knockdown may inhibit this process (Zhong et al., 2013). *Yap1*'s importance in osteoblast proliferation and differentiation, as evidenced by previous studies (Li et al., 2021; Dupont et al., 2011; Pan et al., 2018; Kegelman et al., 2018; Lorthongpanich et al., 2019), aligns with our observation of impaired osteogenesis upon *Yap1* depletion. As a

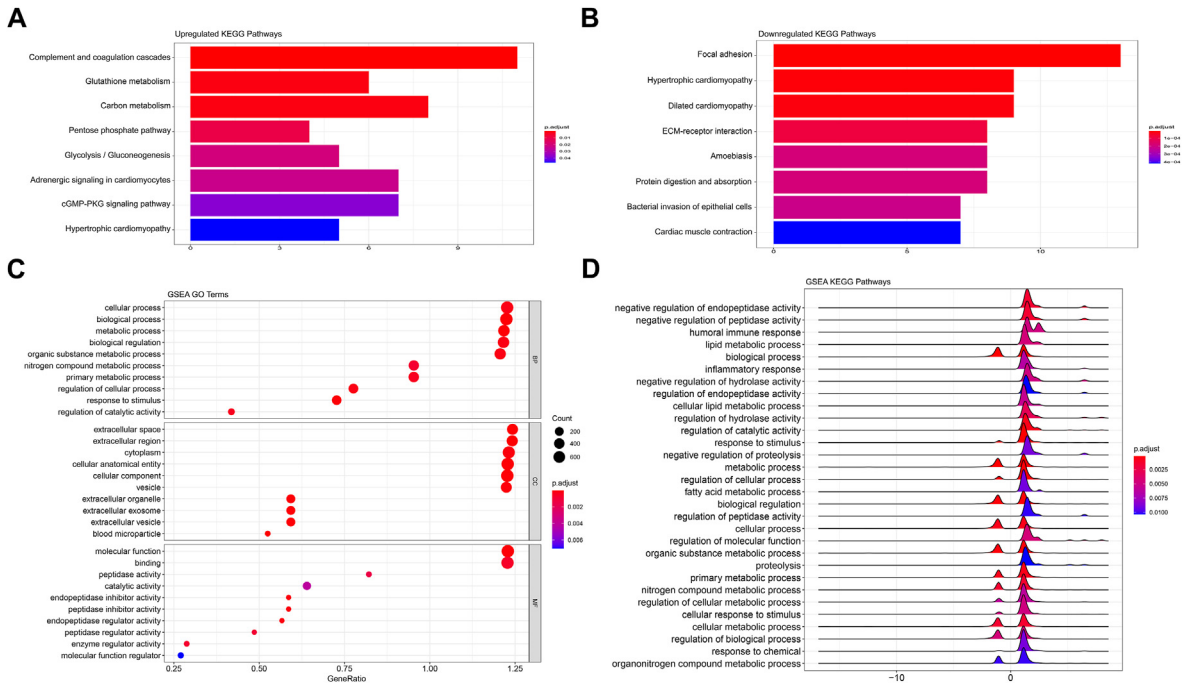

Fig. 5. KEGG and gene ontology analyses of identified proteins. (A) Enriched KEGG pathways by upregulated proteins in *YAP* knocked-down samples compared to control group. (B) Enriched KEGG pathways by downregulated proteins in *YAP* depleted samples compared to control group. (C) top 10 GO terms enriched by identified proteins using the gene set enrichment analysis. (D) KEGG pathways enriched by the protein list using the gene set enrichment analysis.

transcription regulator, *Yap1* can exert these roles, dependent or independent of RUNX2, interacting with TEAD or SMAD proteins. The connection between YAP1 and RUNX2 in osteogenesis is intriguing. RUNX2, a critical transcription factor in bone formation, is known for promoting osteoblast differentiation and maturation. It has been demonstrated that RUNX2 plays an essential role in embryonic bone development by inducing the transdifferentiation of chondrocytes into osteoblasts through stimulating chondrocyte maturation and inhibiting apoptosis of the terminal hypertrophic chondrocytes (Qin et al., 2020). Likewise, it has a crucial role in bone remodeling via osteoprogenitor proliferation and osteoblast differentiation by regulating target genes related to osteogenesis (Chan et al., 2021). As shown recently, the activation of YAP enhances the transcriptional activity of both TEAD and RUNX2 transcription factors (Bruderer et al., 2014; Ebrahimighaei et al., 2022). Moreover, the increased activity of RUNX2 by increased Yap expression and, conversely, negative regulation of RUNX2 upon decreased Yap expression were documented earlier (Zhong et al., 2013). The YAP1-RUNX2 interaction results in the transcription of numerous genes associated with osteogenesis, including *Osteocalcin*, *Col1a1*, *Osteopontin*, *RANKL*, and *MMP13* (Chan et al., 2021). Although we did not observe a significant change in the mRNA level of *RUNX2* following *Yap1* knockdown, the depletion of *Yap1* disrupts the YAP1 and RUNX2 interaction and their colocalization in the nucleus. The observed defect in bone formation during axolotl limb regeneration may be attributed to the inadequate activation of RUNX2 resulting from the decrease in *Yap1* levels. Further investigations are necessary to clarify this point by assessing the transcriptional activity of RUNX2 in the absence of YAP1 during the regeneration process.

Downstream effects of *Yap1* depletion were also investigated using proteomic analysis. Previous studies have noted changes in muscle-related gene expression during the blastema stage of axolotl limb regeneration, which involves cellular dedifferentiation into stem and progenitor cells (Rao et al., 2009; Sibai et al., 2020), as detected in this study. Furthermore, notably, *Yap1*-KD samples showed enrichment in BPs linked to peptidase activity inhibition, aligning with prior research demonstrating the necessity of peptidase activity for successful regeneration in various species (Dolmatov et al., 2019; Dong et al., 2021; Enos et al., 2019; Pasten et al., 2012; Rinkevich et al., 2007). *Yap1*-depleted animals also enriched immune-related BPs. It has been postulated that the prolonged and over-activated immune system response may cause the scarring and prevent the regeneration program (Aurora and Olson, 2014); therefore, it could be inferred that the heightened immune activity in *Yap1*-depleted samples might contribute to their incomplete and delayed regeneration (Demircan et al., 2020; Sibai et al., 2020).

Moreover, several differentially expressed (DE) proteins identified in our study have established roles in bone formation. Notably, the matrix protease, Cathepsin K (CTSK), crucial for bone homeostasis, is positively regulated by YAP (Kegelman et al., 2020), and in our data, its level was lower in *Yap1*-depleted samples. FXIII, a factor in bone healing, exhibited decreased levels following *Yap1* suppression (Kleber et al., 2022). Similarly, Apolipoprotein-E, an osteoclastogenesis inhibitor, was diminished in *Yap1* deficient organisms, possibly leading to increased osteoclast differentiation (Kim et al., 2013; Niemeier et al., 2012). Furthermore, *ATP6V1H*, a component of vacuolar ATPase linked to bone resorption and osteoblast activity, was also downregulated (Duan et al., 2016; Zhang et al., 2017). Additionally, we observed significant dysregulation in the extracellular matrix (ECM) components and related enzymes following YAP1 inhibition in axolotl limb regeneration. This aligns with previous findings emphasizing ECM stiffness in lineage specification and YAP/TAZ activity regulation (Dupont et al., 2011; Engler et al., 2006; Han et al., 2019). Lower levels of crucial ECM components such as collagen types, *tenascin*, *TGFBI*, *decorin*, and *vinculin* were found in *Yap1*-depleted samples. These molecules are essential in various stages of bone formation and osteogenesis, and their reduction may contribute to the observed defective regeneration (Li et al., 2016; Sato et al., 2016; Thapa et al., 2007; Yu et al., 2012b; Kirby and Young, 2018; Zhou et al., 2019).

Among them, as a key component of focal adhesions, vinculin participates in transducing mechanical stimuli into biochemical signals within cells. The binding of the YAP1-TEAD complex to DNA promotes the transcription of focal adhesion signaling and ECM-related genes, such as *α-catenin*, *β-catenin*, *vinculin*, and *CTGF*, in addition to cell cycle and

anti-apoptotic genes (Totaro et al., 2018). Through β-catenin activation, Vinculin enhances the expression of genes associated with osteogenesis, specifically via the β-catenin-CBP-LEF1 complex (Peng et al., 2010; Baron and Kneissel, 2013). Thus, YAP1, as a master regulator, might regulate osteogenesis in axolotl limb regeneration through RUNX2 independent signaling pathway, which should be addressed in future studies.

In summary, our study presents novel findings regarding the regenerative defects resulting from *Yap1* depletion. The data obtained in our study suggest that the hindered bone formation observed in *Yap1* knockdown animals may be attributed to various factors, including increased immune system activity, downregulation of peptidases, changes in ECM composition, altered expression levels of proteins crucial for osteogenesis, and impaired YAP1-RUNX2 activity. However, further investigation is required to comprehensively elucidate the specific roles of these candidate genes in osteogenesis during limb regeneration to obtain a more precise understanding.

5. Conclusion

This study aimed to investigate the role of the YAP1 protein in axolotl limb regeneration. Our findings revealed that the expression level of *Yap1* is higher in neotenic axolotls compared to metamorphic animals during the early stages of limb regeneration. Moreover, the essential role of YAP1 in this regeneration process was evident through the manifestation of bone formation defects upon *Yap1* depletion. The disruption of the YAP1-RUNX2 complex may provide a plausible explanation for the observed deficiency in bone formation. We also employed a proteomics approach to examine the pathways affected by Yap1 inhibition, which may contribute to elucidating the observed defects in axolotl limb regeneration. The analysis of differentially regulated proteins in *Yap1* knockdown samples shed light on altered pathways that could provide insights into the mechanisms underlying the observed regeneration defects. Further investigations involving the modulation of expression levels or activity of the candidate proteins identified in this study, as well as the examination of YAP1-RUNX2-mediated gene expression during axolotl limb regeneration, may help bridge the gap in our understanding of the compromised bone regeneration observed upon *Yap1* depletion.

Funding

This study was supported by the Scientific and Technological Research Council of Turkey (TÜBİTAK) under project number 119Z976, and by the BAGEP Award of the Science Academy.

Author contributions

S.B.: Provision of study material, Collection and assembly of data, Data analysis and interpretation, Manuscript writing, Final approval of manuscript; G.Ö .: Conception and design, Manuscript writing, Final approval of manuscript; N.E.: Conception and design, Manuscript writing, Final approval of manuscript; T.D.: Conception and design, Provision of study material, Collection and assembly of data, Data analysis and interpretation, Manuscript writing, Final approval of manuscript.

Data availability

Data will be made available on request.

Acknowledgements

We thank Ecem Yelkenci, Elif Özbay, Pelin Tuğlu, and Sultan Gül for their help in proteomics experiments and animal care.

Appendix A. Supplementary data

Supplementary data to this article can be found online at https://doi.org/10.1016/j.ydbio.2023.06.001.

References

Aurora, A.B., Olson, E.N., 2014. Immune modulation of stem cells and regeneration. Cell Stem Cell 15, 14–25.
Bai, H., Zhang, N., Xu, Y., Chen, Q., Khan, M., Potter, J.J., Nayar, S.K., Cornish, T., Alpini, G., Bronk, S., Pan, D., Anders, R.A., 2012. Yes-associated protein regulates the hepatic response after bile duct ligation. Hepatology 56, 1097–1107.
Baron, R., Kneissel, M., 2013. WNT signaling in bone homeostasis and disease: from human mutations to treatments. Nat. Med. 19, 179–192.
Beck, C.W., Izpisua Belmonte, J.C., Christen, B., 2009. Beyond early development: Xenopus as an emerging model for the study of regenerative mechanisms. Dev. Dynam. 238, 1226–1248.
Benhamouche, S., Curto, M., Saotome, I., Gladden, A.B., Liu, C.H., Giovannini, M., McClatchey, A.I., 2010. Nf2/Merlin controls progenitor homeostasis and tumorigenesis in the liver. Genes Dev. 24, 1718–1730.
Bruderer, M., Richards, R.G., Alini, M., Stoddart, M.J., 2014. Role and regulation of RUNX2 in osteogenesis. Eur. Cell. Mater. 28, 269–286.
Cai, J., Zhang, N., Zheng, Y., de Wilde, R.F., Maitra, A., Pan, D., 2010. The Hippo signaling pathway restricts the oncogenic potential of an intestinal regeneration program. Genes Dev. 24, 2383–2388.
Camargo, F.D., Gokhale, S., Johnnidis, J.B., Fu, D., Bell, G.W., Jaenisch, R., Brummelkamp, T.R., 2007. YAP1 increases organ size and expands undifferentiated progenitor cells. Curr. Biol. : CB 17, 2054–2060.
Carbonell, M.B., Cardona, J.Z., Delgado, J.P., 2021. Hydrogen peroxide is necessary during tail regeneration in juvenile axolotl. Dev. Dynam. 251, 1054–1076.
Cevik, O., Baykal, A.T., Sener, A., 2016. Platelets proteomic profiles of acute ischemic stroke patients. PLoS One 11, e0158287.
Chan, W.C.W., Tan, Z., To, M.K.T., Chan, D., 2021. Regulation and role of transcription factors in osteogenesis. Int. J. Mol. Sci. 22, 5445.
Demircan, T., Berezikov, E., 2013. The Hippo pathway regulates stem cells during homeostasis and regeneration of the flatworm Macrostomum lignano. Stem Cell. Dev. 22, 2174–2185.
Demircan, T., Hacibektasoglu, H., Sibai, M., Fescioglu, E.C., Altuntas, E., Ozturk, G., Suzek, B.E., 2020. Preclinical molecular signatures of spinal cord functional restoration: optimizing the metamorphic axolotl (Ambystoma mexicanum) model in regenerative medicine. OMICS 24, 370–378.
Demircan, T., Ilhan, A.E., Ovezmyradov, G., Ozturk, G., Yildirim, S., 2019. Longitudinal 16S rRNA data derived from limb regenerative tissue samples of axolotl Ambystoma mexicanum. Sci. Data 6, 70.
Demircan, T., Keskin, I., Dumlu, S.N., Ayturk, N., Avsaroglu, M.E., Akgun, E., Ozturk, G., Baykal, A.T., 2017. Detailed tail proteomic analysis of axolotl (Ambystoma mexicanum) using an mRNA-seq reference database. Proteomics 17, 1600338.
Demircan, T., Ovezmyradov, G., Yildirim, B., Keskin, I., Ilhan, A.E., Fescioglu, E.C., Ozturk, G., Yildirim, S., 2018. Experimentally induced metamorphosis in highly regenerative axolotl (ambystoma mexicanum) under constant diet restructures microbiota. Sci. Rep. 8, 10974.
Dolmatov, I.Y., Shulga, A.P., Ginanova, T.T., Eliseikina, M.G., Lamash, N.E., 2019. Metalloproteinase inhibitor GM6001 delays regeneration in holothurians. Tissue Cell 59, 1–9.
Dong, J., Feldmann, G., Huang, J., Wu, S., Zhang, N., Comerford, S.A., Gayyed, M.F., Anders, R.A., Maitra, A., Pan, D., 2007. Elucidation of a universal size-control mechanism in Drosophila and mammals. Cell 130, 1120–1133.
Dong, Z., Huo, J., Liang, A., Chen, J., Chen, G., Liu, D., 2021. Gamma-Secretase Inhibitor (DAPT), a potential therapeutic target drug, caused neurotoxicity in planarian regeneration by inhibiting Notch signaling pathway. Sci. Total Environ. 781, 146735.
Duan, X., Liu, J., Zheng, X., Wang, Z., Zhang, Y., Hao, Y., Yang, T., Deng, H., 2016. Deficiency of ATP6V1H causes bone loss by inhibiting bone resorption and bone formation through the TGF-β1 pathway. Theranostics 6, 2183–2195.
Dupont, S., Morsut, L., Aragona, M., Enzo, E., Giulitti, S., Cordenonsi, M., Zanconato, F., Le Digabel, J., Forcato, M., Bicciato, S., Elvassore, N., Piccolo, S., 2011. Role of YAP/TAZ in mechanotransduction. Nature 474, 179–183.
Ebrahimighaei, R., Sala-Newby, G.B., Hudson, C., Kimura, T.E., Hathway, T., Hawkins, J., McNeill, M.C., Richardson, R., Newby, A.C., Bond, M., 2022. Combined role for YAP-TEAD and YAP-RUNX2 signalling in substrate-stiffness regulation of cardiac fibroblast proliferation. Biochim. Biophys. Acta Mol. Cell Res. 1869, 119329.
Engler, A.J., Sen, S., Sweeney, H.L., Discher, D.E., 2006. Matrix elasticity directs stem cell lineage specification. Cell 126, 677–689.
Enos, N., Takenaka, H., Scott, S., Salfity, H.V.N., Kirk, M., Egar, M.W., Sarria, D.A., Slayback-Barry, D., Belecky-Adams, T., Chernoff, E.A.G., 2019. Meningeal foam cells and ependymal cells in axolotl spinal cord regeneration. Front. Immunol. 10, 2558.
Galliot, B., Ghila, L., 2010. Cell plasticity in homeostasis and regeneration. Mol. Reprod. Dev. 77, 837–855.
Gregorieff, A., Liu, Y., Inanlou, M.R., Khomchuk, Y., Wrana, J.L., 2015. Yap-dependent reprogramming of Lgr5(+) stem cells drives intestinal regeneration and cancer. Nature 526, 715–718.
Han, P., Frith, J.E., Gomez, G.A., Yap, A.S., O'Neill, G.M., Cooper-White, J.J., 2019. Five piconewtons: the difference between osteogenic and adipogenic fate choice in human mesenchymal stem cells. ACS Nano 13, 11129–11143.

Hayashi, S., Ochi, H., Ogino, H., Kawasumi, A., Kamei, Y., Tamura, K., Yokoyama, H., 2014a. Transcriptional regulators in the Hippo signaling pathway control organ growth in Xenopus tadpole tail regeneration. Dev. Biol. 396, 31–41.
Hayashi, S., Tamura, K., Yokoyama, H., 2014b. Yap1, transcription regulator in the Hippo signaling pathway, is required for Xenopus limb bud regeneration. Dev. Biol. 388, 57–67.
Hayashi, S., Yokoyama, H., Tamura, K., 2015. Roles of Hippo signaling pathway in size control of organ regeneration. Dev. Growth Differ. 57, 341–351.
Heallen, T., Morikawa, Y., Leach, J., Tao, G., Willerson, J.T., Johnson, R.L., Martin, J.F., 2013. Hippo signaling impedes adult heart regeneration. Development 140, 4683–4690.
Johnson, R., Halder, G., 2014. The two faces of Hippo: targeting the Hippo pathway for regenerative medicine and cancer treatment. Nat. Rev. Drug Discov. 13, 63–79.
Juan, W.C., Hong, W., 2016. Targeting the hippo signaling pathway for tissue regeneration and cancer therapy. Genes 7 (9), 55.
Kegelman, C.D., Coulombe, J.C., Jordan, K.M., Horan, D.J., Qin, L., Robling, A.G., Ferguson, V.L., Bellido, T.M., Boerckel, J.D., 2020. YAP and TAZ mediate osteocyte perilacunar/canalicular remodeling. J. Bone Miner. Res. 35, 196–210.
Kegelman, C.D., Mason, D.E., Dawahare, J.H., Horan, D.J., Vigil, G.D., Howard, S.S., Robling, A.G., Bellido, T.M., Boerckel, J.D., 2018. Skeletal cell YAP and TAZ combinatorially promote bone development. Faseb. J. 32, 2706–2721.
Kim, W.S., Kim, H.J., Lee, Z.H., Lee, Y., Kim, H.H., 2013. Apolipoprotein E inhibits osteoclast differentiation via regulation of c-Fos, NFATc1 and NF-kappaB. Exp. Cell Res. 319, 436–446.
Kirby, D.J., Young, M.F., 2018. Isolation, production, and analysis of small leucine-rich proteoglycans in bone. Methods Cell Biol. 143, 281–296.
Kleber, C., Sablotzki, A., Casu, S., Olivieri, M., Thoms, K.M., Horter, J., Schmitt, F.C.F., Birschmann, I., Fries, D., Maegele, M., Schochl, H., Wilhelmi, M., 2022. The impact of acquired coagulation factor XIII deficiency in traumatic bleeding and wound healing. Crit. Care 26, 69.
Kovar, H., Bierbaumer, L., Radic-Sarikas, B., 2020. The YAP/TAZ pathway in osteogenesis and bone sarcoma pathogenesis. Cells 9 (4), 972.
Leigh, N.D., Sessa, S., Dragalzew, A.C., Payzin-Dogru, D., Sousa, J.F., Aggouras, A.N., Johnson, K., Dunlap, G.S., Haas, B.J., Levin, M., Schneider, I., Whited, J.L., 2020. von Willebrand factor D and EGF domains is an evolutionarily conserved and required feature of blastemas capable of multitissue appendage regeneration. Evol. Dev. 22 (4), 297–311.
Li, C., Li, G., Liu, M., Zhou, T., Zhou, H., 2016. Paracrine effect of inflammatory cytokine-activated bone marrow mesenchymal stem cells and its role in osteoblast function. J. Biosci. Bioeng. 121, 213–219.
Li, Y., Wang, J., Zhong, W., 2021. Regulation and mechanism of YAP/TAZ in the mechanical microenvironment of stem cells (Review). Mol. Med. Rep. 24, 506.
Lin, A.Y., Pearson, B.J., 2014. Planarian yorkie/YAP functions to integrate adult stem cell proliferation, organ homeostasis and maintenance of axial patterning. Development 141, 1197–1208.
Loforese, G., Malinka, T., Keogh, A., Baier, F., Simillion, C., Montani, M., Halazonetis, T.D., Candinas, D., Stroka, D., 2017. Impaired liver regeneration in aged mice can be rescued by silencing Hippo core kinases MST1 and MST2. EMBO Mol. Med. 9, 46–60.
Lorthongpanich, C., Thumanu, K., Tangkiettrakul, K., Jiamvoraphong, N., Laowtammathron, C., Damkham, N., Y, U.P., Issaragrisil, S., 2019. YAP as a key regulator of adipo-osteogenic differentiation in human MSCs. Stem Cell Res. Ther. 10, 402.
McCusker, C., Bryant, S.V., Gardiner, D.M., 2015. The axolotl limb blastema: cellular and molecular mechanisms driving blastema formation and limb regeneration in tetrapods. Regeneration 2, 54–71.
McCusker, C., Gardiner, D.M., 2011. The axolotl model for regeneration and aging research: a mini-review. Gerontology 57, 565–571.
Monaghan, J.R., Stier, A.C., Michonneau, F., Smith, M.D., Pasch, B., Maden, M., Seifert, A.W., 2014. Experimentally induced metamorphosis in axolotls reduces regenerative rate and fidelity. Regeneration 1, 2–14.
Moya, I.M., Halder, G., 2018. Hippo-YAP/TAZ signalling in organ regeneration and regenerative medicine. Nat. Rev. Mol. Cell Biol. 20 (4), 211–226.
Niemeier, A., Schinke, T., Heeren, J., Amling, M., 2012. The role of apolipoprotein E in bone metabolism. Bone 50, 518–524.
Nye, H.L., Cameron, J.A., Chernoff, E.A., Stocum, D.L., 2003. Regeneration of the urodele limb: a review. Dev. Dynam. : an official publication of the American Association of Anatomists 226, 280–294.
Pan, J.X., Xiong, L., Zhao, K., Zeng, P., Wang, B., Tang, F.L., Sun, D., Guo, H.H., Yang, X., Cui, S., Xia, W.F., Mei, L., Xiong, W.C., 2018. YAP promotes osteogenesis and suppresses adipogenic differentiation by regulating beta-catenin signaling. Bone Res 6, 18.
Panciera, T., Azzolin, L., Cordenonsi, M., Piccolo, S., 2017. Mechanobiology of YAP and TAZ in physiology and disease. Nat. Rev. Mol. Cell Biol. 18, 758–770.
Pasten, C., Rosa, R., Ortiz, S., Gonzalez, S., Garcia-Arraras, J.E., 2012. Characterization of proteolytic activities during intestinal regeneration of the sea cucumber, Holothuria glaberrima. Int. J. Dev. Biol. 56, 681–691.
Peng, X., Cuff, L.E., Lawton, C.D., DeMali, K.A., 2010. Vinculin regulates cell-surface E-cadherin expression by binding to β-catenin. J. Cell Sci. 123 (4), 567–577.
Qin, X., Jiang, Q., Nagano, K., Moriishi, T., Miyazaki, T., Komori, H., Ito, K., von der Mark, K., Sakane, C., Kaneko, H., 2020. Runx2 is essential for the transdifferentiation of chondrocytes into osteoblasts. PLoS Genet. 16, e1009169.
Rao, N., Jhamb, D., Milner, D.J., Li, B., Song, F., Wang, M., Voss, S.R., Palakal, M., King, M.W., Saranjami, B., Nye, H.L., Cameron, J.A., Stocum, D.L., 2009. Proteomic analysis of blastema formation in regenerating axolotl limbs. BMC Biol. 7, 83.
Rinkevich, Y., Douek, J., Haber, O., Rinkevich, B., Reshef, R., 2007. Urochordate whole body regeneration inaugurates a diverse innate immune signaling profile. Dev. Biol. 312, 131–146.
Rosenkilde, P., Mogensen, E., Centervall, G., Jorgensen, O.S., 1982. Peaks of neuronal membrane antigen and thyroxine in larval development of the Mexican axolotl. Gen. Comp. Endocrinol. 48, 504–514.
Sato, R., Fukuoka, H., Yokohama-Tamaki, T., Kaku, M., Shibata, S., 2016. Immunohistochemical localization of tenascin-C in rat periodontal ligament with reference to alveolar bone remodeling. Anat. Sci. Int. 91, 196–206.
Sibai, M., Altuntas, E., Suzek, B.E., Sahin, B., Parlayan, C., Ozturk, G., Baykal, A.T., Demircan, T., 2020. Comparison of protein expression profile of limb regeneration between neotenic and metamorphic axolotl. Biochem. Biophys. Res. Commun. 522, 428–434.
Sibai, M., Parlayan, C., Tuglu, P., Ozturk, G., Demircan, T., 2019. Integrative analysis of axolotl gene expression data from regenerative and wound healing limb tissues. Sci. Rep. 9, 20280.
Slack, J.M., Lin, G., Chen, Y., 2008. The Xenopus tadpole: a new model for regeneration research. Cell. Mol. Life Sci. : CM 65, 54–63.
Stocum, D.L., 2006. Regenerative Biology and Medicine. Elsevier Academic Press, Amsterdam ; Boston.
Thapa, N., Lee, B.H., Kim, I.S., 2007. TGFBIp/betaig-h3 protein: a versatile matrix molecule induced by TGF-beta. Int. J. Biochem. Cell Biol. 39, 2183–2194.
Totaro, A., Panciera, T., Piccolo, S., 2018. YAP/TAZ upstream signals and downstream responses. Nat. Cell Biol. 20, 888–899.
von Gise, A., Lin, Z., Schlegelmilch, K., Honor, L.B., Pan, G.M., Buck, J.N., Ma, Q., Ishiwata, T., Zhou, B., Camargo, F.D., Pu, W.T., 2012. YAP1, the nuclear target of Hippo signaling, stimulates heart growth through cardiomyocyte proliferation but not hypertrophy. Proc. Natl. Acad. Sci. U.S.A. 109, 2394–2399.
Xin, M., Kim, Y., Sutherland, L.B., Murakami, M., Qi, X., McAnally, J., Porrello, E.R., Mahmoud, A.I., Tan, W., Shelton, J.M., Richardson, J.A., Sadek, H.A., Bassel-Duby, R., Olson, E.N., 2013. Hippo pathway effector Yap promotes cardiac regeneration. Proc. Natl. Acad. Sci. U.S.A. 110, 13839–13844.
Yu, G., Wang, L.G., Han, Y., He, Q.Y., 2012a. clusterProfiler: an R package for comparing biological themes among gene clusters. OMICS 16, 284–287.
Yu, H., Wergedal, J.E., Zhao, Y., Mohan, S., 2012b. Targeted disruption of TGFBI in mice reveals its role in regulating bone mass and bone size through periosteal bone formation. Calcif. Tissue Int. 91, 81–87.
Yui, S., Azzolin, L., Maimets, M., Pedersen, M.T., Fordham, R.P., Hansen, S.L., Larsen, H.L., Guiu, J., Alves, M.R.P., Rundsten, C.F., Johansen, J.V., Li, Y., Madsen, C.D., Nakamura, T., Watanabe, M., Nielsen, O.H., Schweiger, P.J., Piccolo, S., Jensen, K.B., 2018. YAP/TAZ-Dependent reprogramming of colonic epithelium links ECM remodeling to tissue regeneration. Cell Stem Cell 22, 35–49 e37.
Zhang, Y., Huang, H., Zhao, G., Yokoyama, T., Vega, H., Huang, Y., Sood, R., Bishop, K., Maduro, V., Accardi, J., Toro, C., Boerkoel, C.F., Lyons, K., Gahl, W.A., Duan, X., Malicdan, M.C., Lin, S., 2017. ATP6V1H deficiency impairs bone development through activation of MMP9 and MMP13. PLoS Genet. 13, e1006481.
Zhong, W., Tian, K., Zheng, X., Li, L., Zhang, W., Wang, S., Qin, J., 2013. Mesenchymal stem cell and chondrocyte fates in a multishear microdevice are regulated by Yes-associated protein. Stem Cell. Dev. 22, 2083–2093.
Zhou, C., Wang, Q., Zhang, D., Cai, L., Du, W., Xie, J., 2019. Compliant substratum modulates vinculin expression in focal adhesion plaques in skeletal cells. Int. J. Oral Sci. 11, 18.